Effect of Geometry of Shear Connector on the Behavior of Composite Beam - A Numerical Approach

Md. Khasro Miah[1], Md. Rakibul Hasan[1] and AKM Ruhul Amin[1]

[1] Dhaka University of Engineering & Technology, Gazipur, Bangladesh
mkhasro@duet.ac.bd

Abstract. Composite structure is defined as a combination of two or more elements acting together as a single element. The headed stud shear connector in a steel-concrete composite beam generates the composite action by resisting the longitudinal sliding and uplifting between the steel beam and concrete slab. Test results are the key points for research, but working with varying geometric elements is time-consuming and, in some situations, impossible, whereas numerical analysis can easily evaluate the effect of any variation. Using ANSYS software based on the Finite Element Method, numerical analysis has been conducted and verified with the assembled test data. A parametric study examining the geometry variations of shear connectors has been conducted. Three-headed stud shear connectors having a length of 102mm with a stud shank diameter of ϕ16mm, ϕ19mm, and ϕ22mm were considered along with the corresponding head diameter of ϕ25mm, ϕ32mm, and ϕ35mm respectively. The square-headed shear connector has also been introduced to observe the effect of composite action. Based on the analytical result it was found that increasing the diameter of the shear connector gives higher load carrying capacity and stiffness. It is also found that the square-shaped shear connector gives better performance than the circular shear connector in case of resisting slip. Besides the parametric study, the shear distribution of the shear connector along the length has also been investigated.

Keywords*:* *Composite structure, Headed shear connector, ANSYS, Finite Element Method*

1 Introduction

The steel-concrete composite structure has been acknowledged since 1940 as one of the most cost-effective solutions for civil engineering construction in both industrialized and developing nations. This results from reduced structural components, weight savings in steel, and expedited building schedules. The existence of a shear link between the concrete slab and the steel beam influences the behavior of a steel-concrete composite beam. The shear connection inhibits interface sliding and facilitates interaction between the concrete slab and the steel beam. Consequently, compressive and tensile forces are induced in the slab and beam, respectively. Composite action will not occur if the slab is not affixed to the steel beam by shear connectors. In such instances, the

Md.K. Miah et al. (eds.), *Proceedings of the 1st International Conference on Recent Innovation in Civil Engineering and Architecture for Sustainable Development (IICASD 2024)*, Advances in Engineering Research 260,
https://doi.org/10.2991/978-94-6463-672-7_22

impact of the concrete slab can typically be disregarded. The ultimate load of the composite beam is equivalent to the ultimate capacity of the steel beam individually. Several researchers conducted experimental studies on composite beams. The performance of simply supported steel-concrete hybrid beams with corrugated webs under vertical loads was conducted experimentally [1].

The ultimate load of beams with corrugated webs increased by approximately 63% compared to the beam with flat web. The behavior of bolted shear connectors was examined, which exhibited 95% shear resistance in comparison to headed stud shear connectors [2]. In the experimental analysis of steel-concrete composite beams, the impact of high-strength engineering materials on overall flexural responses was investigated [3]. Full-scale composite beam specimens used to investigate the flexural response with multiple connector options as blind bolt and welded stud [4]. The behavior of a composite beam with demountable type shear connectors using push-out tests and composite beam testing done [5]. The effect of shear connections in composite beams was investigated computationally using ANSYS software, and it was found that the deflection of the composite beam was unaffected by the height of the shear connectors [6].

The flexural performance of a hybrid beam with two categories of shear connectors, one being a welded stud and the other being a blind bolt shear connector investigated [7]. The performance of stud-connected steel-concrete hybrid girders was assessed numerically in comparison to experimental work, and it was determined that the FE model predicts a conservative value for the ultimate load [8]. The structural performance of steel-concrete hybrid simply supported beams was modeled numerically by simulating the contact interaction between the surface of the concrete block and the steel joist [9]. Using ANSYS software numerical analysis was carried out and findings were compared to the experimental data [10] to assess the effectiveness of the numerical model. Compressive strength of concrete raised from 20MPa to 70MPa enhanced the load bearing capability of a steel-concrete hybrid beam by approximately 20% [11].

Despite previous studies on shear connectors either experimentally or numerically, there remains a limited understanding of how different geometrical parameters influence the overall performance of composite beams. This research addresses this gap by simulating experimental test results of composite beams using finite element software ANSYS. A parametric study was also carried out after the numerical results well agreed with the previous experimental as well as numerical findings of the steel-concrete hybrid or composite beam.

2 Finite element modeling

2.1 Model Building

The numerical simulation was conducted with pre-defined elements from the ANSYS library. The modeling technique and element selection were derived from the numerical analysis established by Kotinda [9]. The many types of elements pertinent to numerical analysis are delineated in the next section. The numerical simulations created in this work were consistent with the experimental analysis of model beam "A3" carried out by Chapman & Balakrishnan [10]. The geometry of the "A3" beam model is seen in Fig. 1. The beam measures 6050 mm in length, 1220mm in width, and the slab has a thickness of 152mm. The slab is double reinforced, including a steel joist depth of 305 mm and flange widths of 152mm at both the top and bottom. The flange thickness is 18mm, while the web thickness is 10mm.

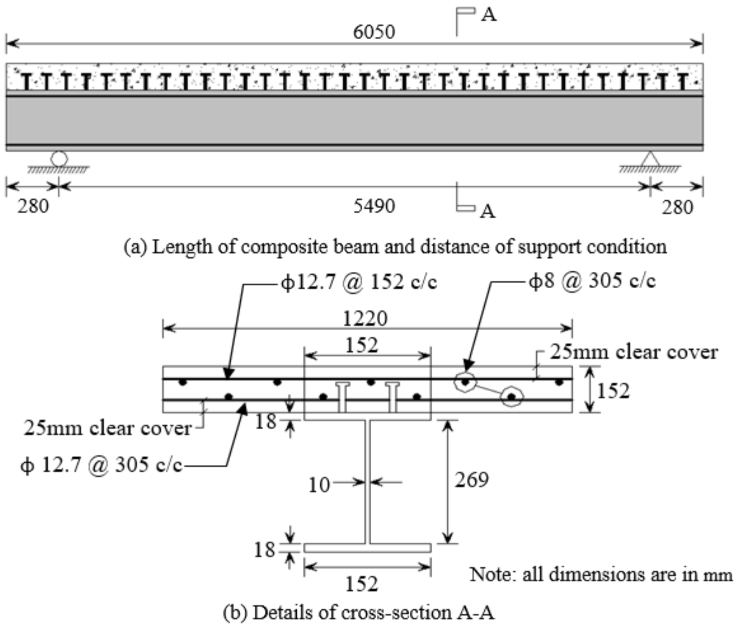

Fig. 1. Geometry of the composite beams

A headed stud shear connector with a diameter of 19mm is utilized in two rows. The total number of shear connectors was 68. The beam is simply supported by a concentrated load at mid-span.

The concrete slab as shown in Fig. 1 was modelled using SOLID 65 element. The element contains eight nodes, with three degrees of freedom for every node and translation in the x, y, and z directions. The steel I-beam is represented using a 4-node shell element (SHELL43), with each node possessing six degrees of freedom. The element encompasses translations and rotations in the nodal x, y, and z axes. The stud shear connector was modelled utilizing the three-node beam element BEAM 189, which possesses six degrees of freedom at each node. The element encompasses rotations and translations along the x, y, and z axes. A bi-linear model incorporating isotropic hardening for shear connectors, grounded in the von Mises criterion. The reinforcing layer has been incorporated as a real constant in the SOLID 65 element. An ideal elasto-plastic model for the reinforcing steel adheres to the von Mises criterion. The material characteristics and volume ratio are specified as actual constants. The volume ratio is determined by dividing the volume of rebar by the total volume of the reinforcing layer.

The TARGE170 and CONTA173 elements facilitate the connection between the slab and the steel beam interface. Upon the contact of two surfaces, pressure is generated, which dissipates to zero upon their separation. In addition to replicating pressure characteristics, this element may also represent the friction and cohesion at the interface between the concrete slab and steel beam. This investigation models only the symmetric half of the beam to minimize the number of elements and reduce processing time. The load was applied in two phases. Initially, the structure's weight was regarded as the gravitational load. In the second step, an external load is applied, concentrated at mid-span between two supports of the composite beam.

2.2 Concrete Materials Modelling

The Mander equations are used to calculate the stress-strain curve of concrete, which is considered to be a uniform isotropic material as shown in Fig. 2. The Equations (1) and (2) define the Mander stress-strain curve for unconfined concrete:

For $\varepsilon_c \leq 2\varepsilon'_c$ (curve portion)

$$f_c = \frac{f'_c\ xr}{r-1+x^r} \tag{1}$$

where

$$x = \frac{\varepsilon_c}{\varepsilon'_c} \quad \text{and} \quad r = \frac{E_c}{E_c - \left(\dfrac{f'_c}{\varepsilon'_c}\right)}$$

For $2\varepsilon'_c < \varepsilon_c \leq \varepsilon_{cu}$ (linear portion)

$$f_c = \left(\frac{2f'_c\ r}{r-1+2^r}\right)\left(\frac{\varepsilon_{cu}-\varepsilon_c}{\varepsilon_{cu}-2\varepsilon'_c}\right) \tag{2}$$

Where r is as defined previously for the curved portion of the curve. f_c= Concrete stress (MPa), ε_c= Concrete strain, E_c= Modulus of elasticity of concrete (MPa), f'_c= Concrete compressive strength (MPa), ε'_c= Concrete strain at f'_c, and ε_{cu}= Ultimate concrete strain capacity.

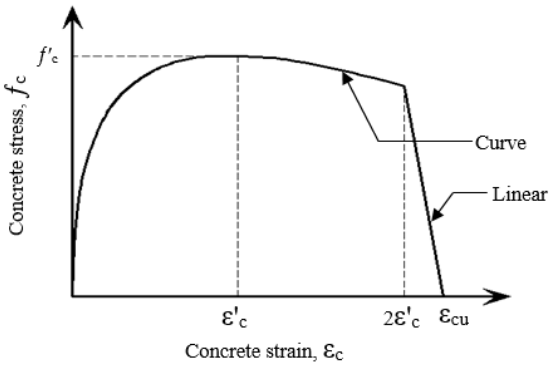

Fig. 2. Mander unconfined stress-strain curve for concrete [12]

2.3 Steel Materials Modelling

The steel yield strain, ε_{sy} is determined from $\varepsilon_{sy} = f_{sy}/E_s$, where, ε_s = Steel strain, f_s = Steel stress (MPa), E_s = Modulus of elasticity of steel (MPa), f_{sy} = Steel yield stress (MPa), f_{su}= Steel maximum stress (MPa), ε_{sh}= Strain at onset of strain hardening, ε_{su}= Strain corresponding to steel maximum stress, ε_r = Strain at steel rupture. The following equations define the simple parametric stress-strain curve for the structural steel.

For $\varepsilon_s \leq \varepsilon_{sy}$ (elastic region),

$$f_s = E_s \varepsilon_s$$

For $\varepsilon_{sy} < \varepsilon_s \leq \varepsilon_{sh}$ (perfectly plastic region)

$$f_s = f_{sy}$$

For $\varepsilon_{sh} < \varepsilon_s \leq \varepsilon_r$ (strain hardening and softening regions)

$$f_s = f_{sy}\left[1 + r\left(\frac{f_{su}}{f_{sy}} - 1\right)e^{(1-r)}\right] \tag{3}$$

where,

$$r = \frac{\varepsilon_s - \varepsilon_{sh}}{\varepsilon_{su} - \varepsilon_{sh}}$$

The equation (3) defines the simple parametric stress-strain curve for the structural steel as shown in Fig. 3.

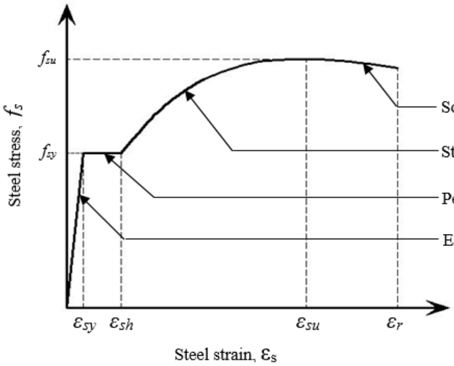

Fig. 3. Structural steel parametric stress-strain curve [13]

2.4 Meshing of Concrete Slab and Steel Joist

In the longitudinal direction (x-axis) the concrete block was divided considering the spacing of shear connectors, as well as ensuring a minimum of two concrete elements between each line of connectors, to observe the change in slip because of the impact of shear connections. In the vertical direction (y-axis) the concrete block is divided in such a way so that each node refers to every connector coincides with a matching node of the concrete block. Furthermore, a layer of elements was created, in terms of reinforcing the top and bottom layers of the concrete block with concrete covering. In transverse direction (z-axis) the concrete block meshing arrangement was set according to the existing nodes belonging to the connectors and the steel profile as shown in Fig. 4.

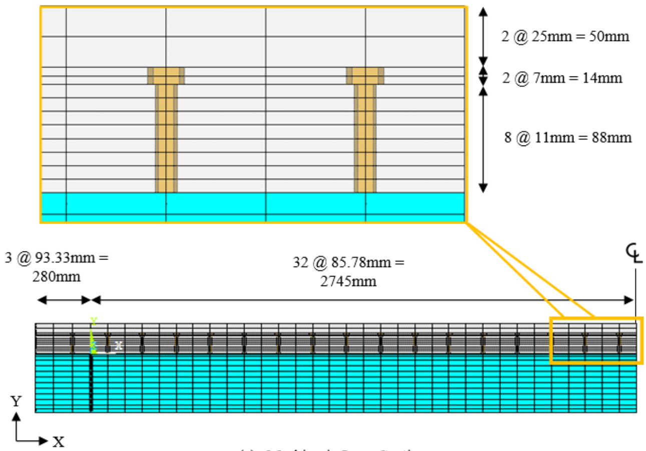

(a) Mashing in Long Section

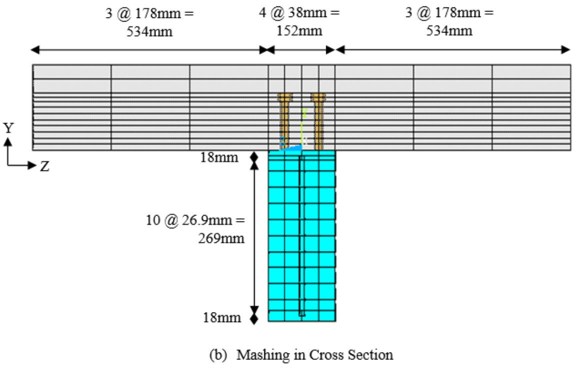

Fig. 4. Meshing of concrete slab and steel joist

3 Numerical Result

The vertical deflection at mid-span under concentrated load was the primary parameter utilized for validating the numerical model; furthermore, the relative end slip of the composite beam was also examined.

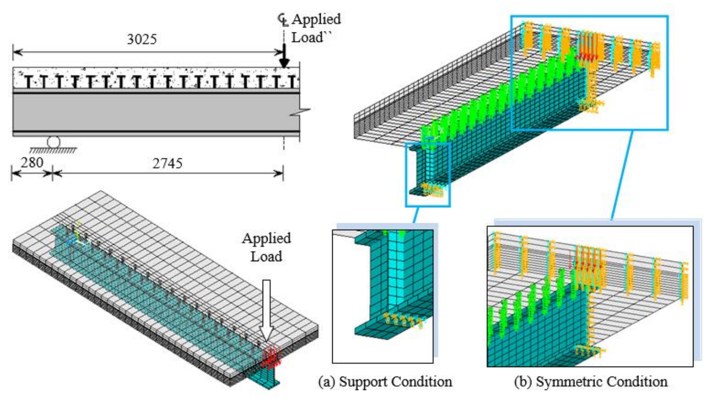

Fig. 5. Symmetric half of the composite beam with single point concentrated load

3.1 Comparison of Numerical Model with Experimental Test Results

The researchers performed numerical evaluations on the same model [9, 11], and Fig. 6 shows that their findings closely match those of this study. The experimental applied load and mid span deflection was investigated [10] also shown along with the numerical results in Fig. 6. In all respect, the numerical load-deflection relations show good agreement with each other numerical as well as experimental relations. The numerical model developed here are utilized for further parametric investigation in the next sections.

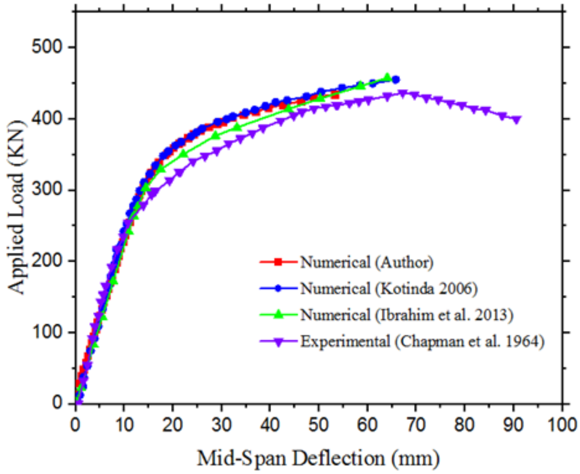

Fig. 6. Load-deflection curves (numerical and experimental)

3.2 Parametric Study

To assess the impact of shear connectors on the performance of composite beams, variations of geometry of the shear connectors are examined, and the same model is analyzed separately, as detailed in the following parametric study.

Effect of Diameter of Shear Connector. The impact of shear connection diameter on the load-deflection behavior of steel-concrete composite beams has been examined by analyzing the composite beam with varying shear connector sizes. The sizes were φ16mm, φ19mm, and φ22mm, with the corresponding stud head diameters being φ25mm, φ32mm, φ35mm, respectively. Table 1 illustrates the impact of shear connector diameter on the behavior of composite beams. Increasing the diameter from φ16mm to φ22mm results in a 5.46% enhancement in ultimate load capacity. The findings demonstrate that maximum loading is achieved for connections with a diameter of φ22mm, exhibiting reduced vertical deflection.

Table 1. Ultimate load variation considering different diameter of shear connectors

Diameter of stud shank (mm), D	Connectors Height (mm), H	Ultimate Load (KN), P_u	Max. Deflection at Ultimate Load (mm), Δu	Load Capacity Variation (%), (P_u/P_{D19}) x100
16	102	420.40	44.53	96.66%
19	102	434.90	53.19	100%
22	102	444.12	61.76	102.12%

The load-deflection curve for various diameters of the shear connector exhibits nearly identical results across both the linear and non-linear ranges, as illustrated in Fig. 7.

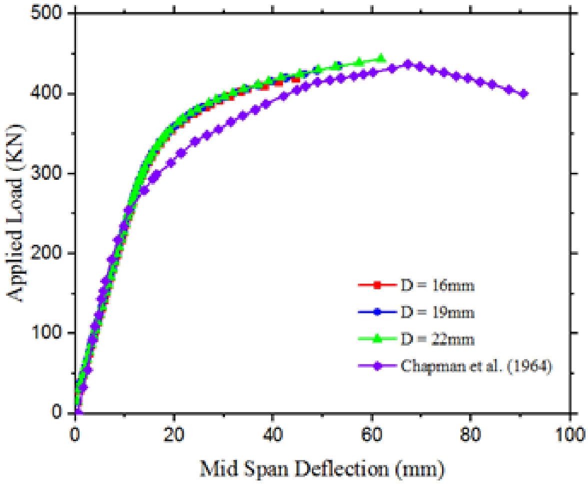

Fig. 7. Load-deflection curves with different diameters of shear connectors

The relative end slip of the composite beam was evaluated utilizing three different diameters of the shear connection, as specified in Table 2. Enhancing the diameter of the shear connector markedly improves the resistance to longitudinal sliding at the interface between the concrete slab and the steel joist. In this study, the φ16mm diameter connector demonstrates inferior values compared to the φ19mm, attributable to its lower ultimate load capacity. Increasing the diameter from φ19mm to φ22mm yields a 26.17% enhancement in slip resistance. Fig. 8 depicts the load versus slip graph of a composite beam using shear connectors of differing diameters.

From the Fig. 8, it is clearly shown that with increasing the diameter of shear connector relative end slip decrease and, in this case, connectors having diameter ϕ22mm shows better result against resisting the end slip. So, from the analysis of the behavior of the composite beam, we can summarize that increasing the diameter of the shear connector will increase the ultimate load-carrying capacity and give a better result against resisting the longitudinal sliding.

Table 2. End slip considering different diameter of shear connectors

Diameter of stud shank (mm), D	Connectors Height (mm), H	Ultimate Load (KN), P_u	End Slip at Ultimate Load (mm), U_x	End Slip Variation (%), (U_x/U_{D19}) x100
16	102	420.40	44.53	96.66%
19	102	434.90	53.19	100%
22	102	444.12	61.76	102.12%

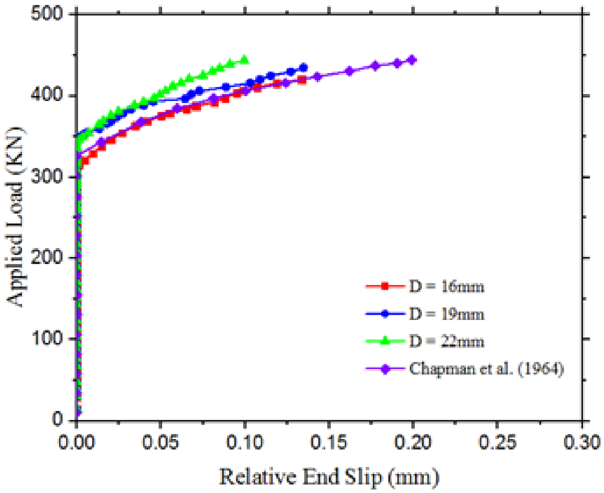

Fig. 8. Load-slip curves with different diameters of shear connectors

Effect of Shape of Shear Connector. To study the effect of shear connector shape on the load-deflection behavior of composite beams, the same model was analyzed with square shear connector. Circular connectors having diameter φ19mm are converted into square shape by keeping the same steel area. The equivalent size of square connectors body considered as 16.83mm with the corresponding connectors head as 28.35mm. All other parameters of shear connectors remain the same as shown in Fig. 9.

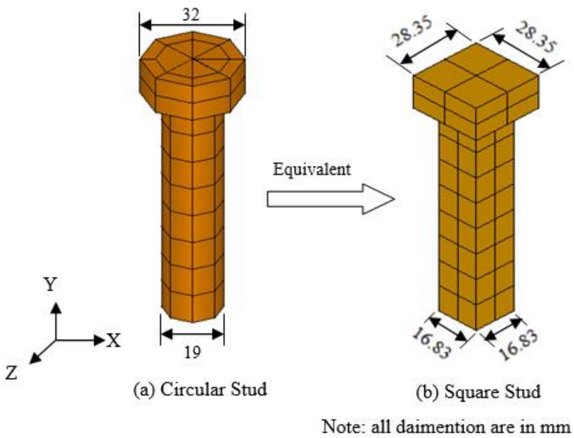

Fig. 9. Dimensions of circular and equivalent square-headed shear connector

The results shown in Table 3 indicate that square shear connections exhibit a little bit more load carrying capability than circular shear connectors. A square-shaped connector measuring 16.83mm×16.83mm is equivalent to a φ19mm circular connector, providing a 0.92% increase in load-carrying capacity. The load-deflection curve indicates that alterations in the configuration of the shear connector have a negligible impact on the behavior of the composite beam, as illustrated in Fig. 10.

Table 3. Load capacity variation considering the different shape of shear connectors

Connectors Shape	Connectors Diameter/size	Connectors Height (mm), H	Ultimate Load (KN), Pu	Max. Deflection at Ultimate Load (mm), Δu	Load Capacity Variation (%), (Pu/Pcir) x100
Circular	φ19	102	434.90	53.19	100%
Square	16.83×16.83	102	438.92	58.75	100.92%

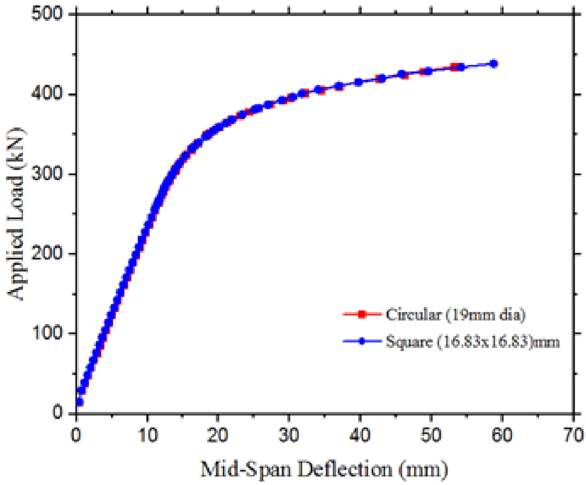

Fig. 10. Load-deflection relations with different shape of shear connectors

The impact of altering the shear connector from circular to square on load-deflection behavior is minimal; nevertheless, the variance in load-relative end slip resulting from these shape modifications holds some significance. The results in Table 4 indicate that, as the ultimate load increases, the slip decreases by 3.50% for the 16.83mm×16.83mm square shear connector in comparison to the φ19mm circular connector. Square connections demonstrate marginally superior performance against resistance, as indicated by the end slip in the load versus slip curve depicted in Fig. 11.

Table 4. End slip variation considering different shape of shear connectors

Connectors Shape	Connectors Diameter/size	Connectors Height (mm), H	Ultimate Load (KN), P_u	End Slip at Ultimate Load (mm), U_x	End Slip Variation (%), (U_x/U_{cir}) x100
Circular	φ19	102	434.90	0.1345	100%

Square	16.83×16.83	102	438.92	0.1298	96.50%

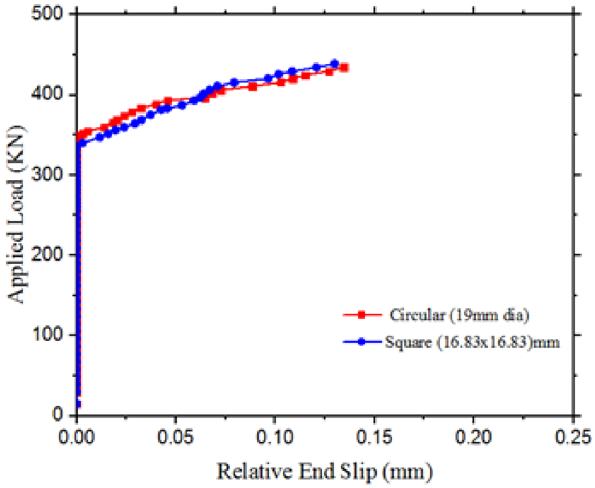

Fig. 11. Load-slip curve with different shape of shear connectors

Variation of Shear Force along the Length of Stud Shear Connector. The bearing forces between the shear connector and the surrounding concrete transmit the shear force applied to the composite system. Fig. 12 illustrates the shear force transmission of a stud shear connector, which one is placed at 1458.3mm from the mid-span. The shear force zero approximately at the mid height of shear connector shank. It is observed from Fig. 12 that for a particular applied load (209.0kN), the lower half of the shank of the connector resists almost negative shear force and the upper half portion resists positive shear force where the connectors head experience negative shear and resists vertical separation. Similarly, for three different applied loads of 305.0kN, 402.0kN and 435.0kN, the shear force distribution along stud shank follows the similar trend with zero shear force at the same location.

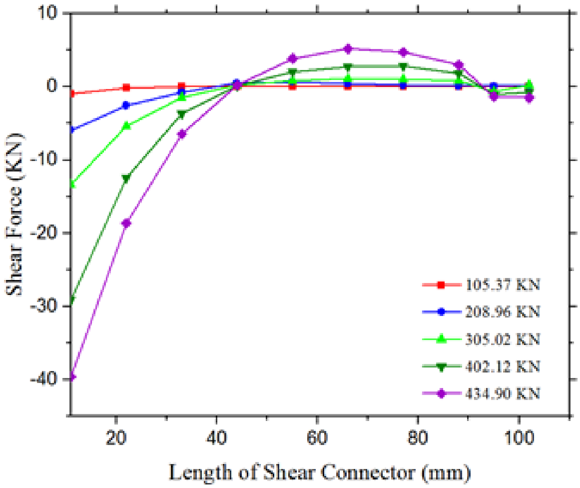

Fig. 12. Shear force distribution along the length of the shear connector

4 CONCLUSIONS

The following are the main conclusions obtained from the results of finite element analysis:

1. The load-deflection are found well agreed with numerical results investigated Kotinda (2006), and Ibrahim et al. (2013). These results demonstrated the accuracy and effectiveness of the developed numerical model;
2. The numerical model well agreed with experimental results [10] in all respect;
3. The load carrying capacity increase by 5.46% and slip decrease by 26.17% with increasing the stud diameter from 16mm to 22mm;
4. Employing an analogous square shear connection (16.83mm x 16.83mm) in place of the traditional stud shear connector (φ19mm) yields a nearly identical load-carrying capacity (0.92% larger) and results in a reduction of relative end slip (3.50% lower);
5. Consequently, taking into account all factors, including load-carrying capacity and resistance to relative end slide, a square-shaped shear connector may be utilized in lieu of a standard circular shear connector.

Acknowledgments. The authors express their profound appreciation to the Department of Civil Engineering, DUET, Gazipur, for their support and collaboration in completing the research effort. This task would not have been accomplished without this unwavering support.

Disclosure of Interests. The authors have no competing interests to declare that are relevant to the content of this article.

References

1. Hafez, A. M. A., Ahmed, M. M., Alamary, A. S., Mohmoud, A. M. (2012). Behavior of simply supported composite concrete-steel beam with corrugated web under vertical loads. *In Journal of Engineering Sciences*, Vol. 40, Issue 1.
2. Loqman, N., Safiee, N. A., Bakar, N. A., Nasir, N. A. M. (2018). Structural behavior of steel-concrete composite beam using bolted shear connectors: a review. MATEC Web of Conferences, 203. https://doi.org/10.1051/matecconf/201820306010.
3. Zhao, H., Yuan, Y. (2010). Experimental studies on composite beams with high-strength steel and concrete. Steel and Composite Structures. 10(5), 373–383.
4. Sameera, W. P., Brian Uy, Mirza O., Zhu X. (2016). Flexural behavior of composite steel-concrete beams utilizing blind bolt shear connectors. Engineering Structures, 114, 181–194. https://doi.org/10.1016/j.engstruct.2016.01.057.
5. Rehman, N. U. (2017). Behavior of demountable shear connectors in composite structures. Faculty of Engineering and Informatics, University of Bradford.
6. Patil, P. S. & Shaikh, M. G. (2013). A Study of effect of shear connector in composite beam in combined bending and shear by ANSYS. In International Journal of Innovative Technology and Exploring Engineering (IJITEE), (Issue 3).
7. Pandilatha, P. & Surumi, R. S. (2017). Comparative study on flexural behavior of steel concrete composite beam using welded and bolted shear connector. International Journal of Civil Engineering and Technology (IJCIET), Volume 8, Issue 5, May 2017, pp. 1016–1024, Article ID: IJCIET_08_05_109.
8. Prakash, A., Anandavalli N., Madheswaran C. K., Rajasankar J., Lakshmanan N. (2011). Three-dimensional FE model of stud connected steel-concrete composite girders subjected to monotonic loading. In International Journal of Mechanics and Applications (Vol. 1, Issue 1). http://journal.sapub.org/mechanics.
9. Kotinda, T. I. (2006). Numerical modeling of steel-concrete composite beams simply supported: emphasis to the study of the slab-beam interface. School of Engineering of São Carlos, University of São Paulo, 116 p.
10. Chapman, J. C., Balakrishnan, S. (1964). Experiments on composite beams. The Structural Engineer, v. 42, p. 369–383.
11. Ibrahim, A. M., Ahmed, Q. W. (2013). Nonlinear analysis of simply supported composite steel-concrete beam. In Diyala Journal of Engineering Sciences, Vol. 06, No. 03, pp. 107-126.
12. Mander, J.B., M.J.N. Priestley, R. Park (1984). Theoretical Stress-Strain Model for Confined Concrete. Journal of Structural Engineering. ASCE. 114(3). 1804-1826.
13. Holzer, S., Melosh, R., Somers, A. E. (1975). SINDER. A Computer Code for General Analysis of Two-Dimensional Reinforced Concrete Structures. Report. AFWL-TR-74-228 Vol. 1. Air Force Weapons Laboratory, Kirtland, AFB, New Mexico.